EUROPEAN ORGANIZATION FOR NUCLEAR RESEARCH

CERN-EP-2001-003
15th January, 2001

A Search for a Radial Excitation of the $D^{*\pm}$ Meson

The OPAL Collaboration

Abstract

A sample of 3.73 million hadronic Z decays, recorded with the OPAL detector at LEP in the years 1991–95, has been used to search for a narrow resonance corresponding to the decay of the $D^{*\prime\pm}(2629)$ meson into $D^{*\pm}\pi^+\pi^-$. The D^{*+} mesons are reconstructed in the decay channel $D^{*+} \to D^0\pi^+$ with $D^0 \to K^-\pi^+$. No evidence for a narrow $D^{*\prime\pm}(2629)$ resonance is found. A limit on the production of $D^{*\prime\pm}(2629)$ in hadronic Z decays is derived:

$$f(Z \to D^{*\prime\pm}(2629)) \times \mathrm{Br}(D^{*\prime+} \to D^{*+}\pi^+\pi^-) < 3.1 \times 10^{-3} \quad (95\%\ \mathrm{C.L.})$$

(Submitted to Euro. Phys. J C)

The OPAL Collaboration

G. Abbiendi[2], C. Ainsley[5], P.F. Åkesson[3], G. Alexander[22], J. Allison[16], G. Anagnostou[1], K.J. Anderson[9], S. Arcelli[17], S. Asai[23], D. Axen[27], G. Azuelos[18,a], I. Bailey[26], A.H. Ball[8], E. Barberio[8], R.J. Barlow[16], R.J. Batley[5], T. Behnke[25], K.W. Bell[20], G. Bella[22], A. Bellerive[9], G. Benelli[2], S. Bethke[32], O. Biebel[32], I.J. Bloodworth[1], O. Boeriu[10], P. Bock[11], J. Böhme[25], D. Bonacorsi[2], M. Boutemeur[31], S. Braibant[8], L. Brigliadori[2], R.M. Brown[20], H.J. Burckhart[8], J. Cammin[3], P. Capiluppi[2], R.K. Carnegie[6], B. Caron[28], A.A. Carter[13], J.R. Carter[5], C.Y. Chang[17], D.G. Charlton[1,b], P.E.L. Clarke[15], E. Clay[15], I. Cohen[22], J. Couchman[15], A. Csilling[15,i], M. Cuffiani[2], S. Dado[21], G.M. Dallavalle[2], S. Dallison[16], A. De Roeck[8], E.A. De Wolf[8], P. Dervan[15], K. Desch[25], B. Dienes[30,f], M.S. Dixit[7], M. Donkers[6], J. Dubbert[31], E. Duchovni[24], G. Duckeck[31], I.P. Duerdoth[16], P.G. Estabrooks[6], E. Etzion[22], F. Fabbri[2], M. Fanti[2], L. Feld[10], P. Ferrari[12], F. Fiedler[8], I. Fleck[10], M. Ford[5], A. Frey[8], A. Fürtjes[8], D.I. Futyan[16], P. Gagnon[12], J.W. Gary[4], G. Gaycken[25], C. Geich-Gimbel[3], G. Giacomelli[2], P. Giacomelli[8], D. Glenzinski[9], J. Goldberg[21], C. Grandi[2], K. Graham[26], E. Gross[24], J. Grunhaus[22], M. Gruwé[08], P.O. Günther[3], A. Gupta[9], C. Hajdu[29], G.G. Hanson[12], K. Harder[25], A. Harel[21], M. Harin-Dirac[4], M. Hauschild[8], C.M. Hawkes[1], R. Hawkings[8], R.J. Hemingway[6], C. Hensel[25], G. Herten[10], R.D. Heuer[25], J.C. Hill[5], K. Hoffman[8], R.J. Homer[1], A.K. Honma[8], D. Horváth[29,c], K.R. Hossain[28], R. Howard[27], P. Hüntemeyer[25], P. Igo-Kemenes[11], K. Ishii[23], A. Jawahery[17], H. Jeremie[18], C.R. Jones[5], P. Jovanovic[1], T.R. Junk[6], N. Kanaya[23], J. Kanzaki[23], G. Karapetian[18], D. Karlen[6], V. Kartvelishvili[16], K. Kawagoe[23], T. Kawamoto[23], R.K. Keeler[26], R.G. Kellogg[17], B.W. Kennedy[20], D.H. Kim[19], K. Klein[11], A. Klier[24], S. Kluth[32], T. Kobayashi[23], M. Kobel[3], T.P. Kokott[3], S. Komamiya[23], R.V. Kowalewski[26], T. Kämer[25], T. Kress[4], P. Krieger[6], J. von Krogh[11], D. Krop[12], T. Kuhl[3], M. Kupper[24], P. Kyberd[13], G.D. Lafferty[16], H. Landsman[21], D. Lanske[14], I. Lawson[26], J.G. Layter[4], A. Leins[31], D. Lellouch[24], J. Letts[12], L. Levinson[24], R. Liebisch[11], J. Lillich[10], C. Littlewood[5], A.W. Lloyd[1], S.L. Lloyd[13], F.K. Loebinger[16], G.D. Long[26], M.J. Losty[7], J. Lu[27], J. Ludwig[10], A. Macchiolo[18], A. Macpherson[28,l], W. Mader[3], S. Marcellini[2], T.E. Marchant[16], A.J. Martin[13], J.P. Martin[18], G. Martinez[17], T. Mashimo[23], P. Mättig[24], W.J. McDonald[28], J. McKenna[27], T.J. McMahon[1], R.A. McPherson[26], F. Meijers[8], P. Mendez-Lorenzo[31], W. Menges[25], F.S. Merritt[9], H. Mes[7], A. Michelini[2], S. Mihara[23], G. Mikenberg[24], D.J. Miller[15], W. Mohr[10], A. Montanari[2], T. Mori[23], K. Nagai[13], I. Nakamura[23], H.A. Neal[33], R. Nisius[8], S.W. O'Neale[1], F.G. Oakham[7], F. Odorici[2], A. Oh[8], A. Okpara[11], M.J. Oreglia[9], S. Orito[23], C. Pahl[32], G. Pásztor[8,i], J.R. Pater[16], G.N. Patrick[20], J.E. Pilcher[9], J. Pinfold[28], D.E. Plane[8], B. Poli[2], J. Polok[8], O. Pooth[8], A. Quadt[8], K. Rabbertz[8], C. Rembser[8], P. Renkel[24], H. Rick[4], N. Rodning[28], J.M. Roney[26], S. Rosati[3], K. Roscoe[16], A.M. Rossi[2], Y. Rozen[21], K. Runge[10], O. Runolfsson[8], D.R. Rust[12], K. Sachs[6], T. Saeki[23], O. Sahr[31], E.K.G. Sarkisyan[8,m], C. Sbarra[26], A.D. Schaile[31], O. Schaile[31], P. Scharff-Hansen[8], M. Schröder[8], M. Schumacher[25], C. Schwick[8], W.G. Scott[20], R. Seuster[14,g], T.G. Shears[8,j], B.C. Shen[4], C.H. Shepherd-Themistocleous[5], P. Sherwood[15], G.P. Siroli[2], A. Skuja[17], A.M. Smith[8], G.A. Snow[17], R. Sobie[26], S. Söldner-Rembold[10,e], S. Spagnolo[20], F. Spano[9], M. Sproston[20], A. Stahl[3], K. Stephens[16], D. Strom[19], R. Ströhmer[31], L. Stumpf[26], B. Surrow[8], S.D. Talbot[1], S. Tarem[21], M. Tasevsky[8], R.J. Taylor[15], R. Teuscher[9], J. Thomas[15], M.A. Thomson[5], E. Torrence[9], S. Towers[6], D. Toya[23], T. Trefzger[31], I. Trigger[8], Z. Trócsányi[30,f], E. Tsur[22], M.F. Turner-Watson[1], I. Ueda[23], B. Vachon[26], C.F. Vollmer[31], P. Vannerem[10], M. Verzocchi[8], H. Voss[8], J. Vossebeld[8], D. Waller[6], C.P. Ward[5], D.R. Ward[5], P.M. Watkins[1], A.T. Watson[1], N.K. Watson[1], P.S. Wells[8],

T. Wengler[8], N. Wermes[3], D. Wetterling[11] J.S. White[6], G.W. Wilson[16], J.A. Wilson[1], T.R. Wyatt[16], S. Yamashita[23], V. Zacek[18], D. Zer-Zion[8,k]

[1]School of Physics and Astronomy, University of Birmingham, Birmingham B15 2TT, UK
[2]Dipartimento di Fisica dell' Università di Bologna and INFN, I-40126 Bologna, Italy
[3]Physikalisches Institut, Universität Bonn, D-53115 Bonn, Germany
[4]Department of Physics, University of California, Riverside CA 92521, USA
[5]Cavendish Laboratory, Cambridge CB3 0HE, UK
[6]Ottawa-Carleton Institute for Physics, Department of Physics, Carleton University, Ottawa, Ontario K1S 5B6, Canada
[7]Centre for Research in Particle Physics, Carleton University, Ottawa, Ontario K1S 5B6, Canada
[8]CERN, European Organisation for Nuclear Research, CH-1211 Geneva 23, Switzerland
[9]Enrico Fermi Institute and Department of Physics, University of Chicago, Chicago IL 60637, USA
[10]Fakultät für Physik, Albert Ludwigs Universität, D-79104 Freiburg, Germany
[11]Physikalisches Institut, Universität Heidelberg, D-69120 Heidelberg, Germany
[12]Indiana University, Department of Physics, Swain Hall West 117, Bloomington IN 47405, USA
[13]Queen Mary and Westfield College, University of London, London E1 4NS, UK
[14]Technische Hochschule Aachen, III Physikalisches Institut, Sommerfeldstrasse 26-28, D-52056 Aachen, Germany
[15]University College London, London WC1E 6BT, UK
[16]Department of Physics, Schuster Laboratory, The University, Manchester M13 9PL, UK
[17]Department of Physics, University of Maryland, College Park, MD 20742, USA
[18]Laboratoire de Physique Nucléaire, Université de Montréal, Montréal, Quebec H3C 3J7, Canada
[19]University of Oregon, Department of Physics, Eugene OR 97403, USA
[20]CLRC Rutherford Appleton Laboratory, Chilton, Didcot, Oxfordshire OX11 0QX, UK
[21]Department of Physics, Technion-Israel Institute of Technology, Haifa 32000, Israel
[22]Department of Physics and Astronomy, Tel Aviv University, Tel Aviv 69978, Israel
[23]International Centre for Elementary Particle Physics and Department of Physics, University of Tokyo, Tokyo 113-0033, and Kobe University, Kobe 657-8501, Japan
[24]Particle Physics Department, Weizmann Institute of Science, Rehovot 76100, Israel
[25]Universität Hamburg/DESY, II Institut für Experimental Physik, Notkestrasse 85, D-22607 Hamburg, Germany
[26]University of Victoria, Department of Physics, P O Box 3055, Victoria BC V8W 3P6, Canada
[27]University of British Columbia, Department of Physics, Vancouver BC V6T 1Z1, Canada
[28]University of Alberta, Department of Physics, Edmonton AB T6G 2J1, Canada
[29]Research Institute for Particle and Nuclear Physics, H-1525 Budapest, P O Box 49, Hungary
[30]Institute of Nuclear Research, H-4001 Debrecen, P O Box 51, Hungary
[31]Ludwigs-Maximilians-Universität München, Sektion Physik, Am Coulombwall 1, D-85748 Garching, Germany
[32]Max-Planck-Institute für Physik, Föhring Ring 6, 80805 München, Germany
[33]Yale University,Department of Physics,New Haven, CT 06520, USA

[a] and at TRIUMF, Vancouver, Canada V6T 2A3
[b] and Royal Society University Research Fellow
[c] and Institute of Nuclear Research, Debrecen, Hungary
[e] and Heisenberg Fellow
[f] and Department of Experimental Physics, Lajos Kossuth University, Debrecen, Hungary
[g] and MPI München
[i] and Research Institute for Particle and Nuclear Physics, Budapest, Hungary
[j] now at University of Liverpool, Dept of Physics, Liverpool L69 3BX, UK
[k] and University of California, Riverside, High Energy Physics Group, CA 92521, USA
[l] and CERN, EP Div, 1211 Geneva 23
[m] and Tel Aviv University, School of Physics and Astronomy, Tel Aviv 69978, Israel.

1 Introduction

Quark models based on Quantum Chromodynamics (QCD) [1, 2] predict the existence of charm mesons whose radial wave functions are not in their ground state. A spin doublet containing a pseudoscalar 2^1S_0 and a vector 2^3S_1 state is expected. These states are referred to as the D' and $D^{*\prime}$, respectively. Their masses are predicted to be $m_{D'} = 2.579\ \mathrm{GeV}/c^2$ and $m_{D^{*\prime}} = 2.629\ \mathrm{GeV}/c^2$ [2] (see Table 1). The uncertainty on these masses is estimated to be of the order of 20 MeV/c^2 from the difference between the values obtained in computations [2] and observations [3] of the masses of orbitally excited states.

The kinematically favoured decay mode of the $D^{*\prime +}$ is presumed to be the direct three-body decay into a $D^{*+}\pi^+\pi^-$ final state[1]. This is an S-wave decay and thus generally expected to be broad, although a model exists [4] which estimates the partial width of this decay mode to be less than 1 MeV/c^2. Decays via an intermediate orbitally excited D meson could also contribute to the same final state; these decay widths are estimated to be several MeV/c^2 by the same model. If enough phase space is available, $D^{*\prime +}$ decays to a $D^{*+}\rho$ state with $\rho \to \pi^+\pi^-$ might also be allowed. The decays via orbitally excited states include S-wave ($D^{*\prime +} \to D_1^{\prime 0}\pi^+$, $D_1^{\prime 0} \to D^{*+}\pi^-$), and D-wave transitions (e.g. $D^{*\prime +} \to D_2^{*0}\pi^+$, $D_2^{*0} \to D^{*+}\pi^-$). The decays involving a ρ are P-wave transitions. The higher partial waves are expected to be suppressed due to lack of phase space.

state	J_j^P	predicted mass [GeV/c^2] [2]	observed properties [3]	
			mass [GeV/c^2]	width [MeV/c^2]
D	$0^-_{1/2}$	1.875	1.865	
D^*	$1^-_{1/2}$	2.009	2.010	< 0.131
D_0^*	$0^+_{1/2}$	2.438	} (2.461) [5]	(290) [5]
D_1^*	$1^+_{1/2}$	2.501		
D_1	$1^+_{3/2}$	2.414	2.422	18.9
D_2^*	$2^+_{3/2}$	2.459	2.459	23
D'	$0^-_{1/2}$	2.579		
$D^{*\prime}$	$1^-_{1/2}$	2.629	(2.637) [6]	(< 15) [6]

Table 1: Masses of charm mesons as predicted in Ref. [2]. Measurements of the meson masses and width are given where available [3]. Values in brackets are not from Ref. [3], but represent recent observations from CLEO [5] and DELPHI [6]. D_0^*, D_1^*, D_1, and D_2^* are orbital excitations (the D_1^* meson is also known as D_1'). D' and $D^{*\prime}$ are radial excitations.

The only experimental evidence for the existence of radially excited D mesons comes from the DELPHI collaboration which has published an observation of a narrow resonance decaying to $D^{*+}\pi^+\pi^-$ [6]. The observed mass of $2.637 \pm 0.002(\mathrm{stat.}) \pm 0.006(\mathrm{syst.})\ \mathrm{GeV}/c^2$ is close to the theoretical prediction. However, the interpretation of this D resonance as $D^{*\prime}$ is controversial, since the narrow width is incompatible with most theoretical models [7]. The DELPHI measurement of the width of the state is limited by their detector resolution and quoted to be smaller than 15 MeV/c^2 at 95% C.L.

[1] Charge conjugates will be implied throughout this paper.

This paper presents a search for the state reported by DELPHI in hadronic Z decays recorded with the OPAL detector. The search covers both the region of the resonance measured by DELPHI as well as any other narrow resonance in the vicinity of the predicted $D^{*\prime\pm}$ mass. Therefore the particle being searched for will be referred to as $D^{*\prime\pm}(2629)$ throughout this paper.

After a description of the data and Monte Carlo samples, the selection criteria for the $D^{*\prime+}$ mesons are presented. Since the production mechanism of $D^{*\prime+}$ mesons is different in $Z \to b\overline{b}$ and $Z \to c\overline{c}$ events, two different selections are used to reconstruct $D^{*\prime+}$ mesons. One is optimized to select $D^{*\prime+}$ candidates in primary b-events using vertex information, while the second selection uses harder cuts on the momentum of the $D^{*\prime+}$ candidate, resulting in a sample enhanced in $c\overline{c}$ events. In Section 5, the selection results for data and Monte Carlo events are presented. Systematic checks are discussed subsequently, and the calculation of limits on the production rate is described in Section 7. In the concluding Section our results are compared with those published by DELPHI [6].

2 The OPAL Detector and Event Simulation

A detailed description of the OPAL detector can be found elsewhere [8]. The most important components of the detector for this analysis are the silicon microvertex detector, the tracking chambers and the electromagnetic calorimeter. The microvertex detector consists of two layers of silicon strip detectors which provide high spatial resolution near the interaction region. The central jet chamber is optimized for good spatial resolution in the plane perpendicular to the beam axis[2]. The resolution along the beam direction is improved by the z information delivered by the silicon microvertex detector, by a vertex detector between the silicon detector and the main tracking chambers, and by z-chambers surrounding the main tracking chamber. The central detector provides precise determination of momenta of charged particles by measuring the curvature of their trajectories in a magnetic field of 0.435 T. The solenoid is mounted outside the tracking chambers but inside the electromagnetic calorimeter, which consists of approximately 12 000 lead glass blocks providing an azimuthal coverage up to polar angles of $|\cos\theta| < 0.98$. To improve the shower energy and spatial resolution, a preshower detector (presampler) is mounted between the solenoid and the electromagnetic calorimeter.

For background studies, about 8 million hadronic decays of the Z have been simulated using the JETSET 7.4 Monte Carlo [9] with parameters tuned to the OPAL data [10]. In addition, samples with simulated $D^{*\prime}$ decays have been generated since JETSET does not include $D^{*\prime}$ production by default. For the production of the $D^{*\prime}$ Monte Carlo samples with JETSET, radially excited D meson states have been implemented into JETSET with the mass set to 2.629 GeV/c^2, according to the most recent calculation [2], and the width set to zero. The possible effects of a non-zero width are treated later as systematic uncertainty. DELPHI only measured the ratio of the $D^{*\prime+}$ and $D_J^{(*)0}$ production rates[3] [6], and therefore this measurement

[2]The OPAL coordinate system is defined as a right-handed Cartesian coordinate system, with the x-axis pointing in the plane of the LEP collider towards the centre of the ring and the z-axis along the electron beam direction.

[3]The symbol $D_J^{(*)}$ represents the two narrow orbital resonances D_1 and D_2^*.

has been combined with the OPAL measurement of $D_J^{(*)0}$ production [11] to calculate the expected absolute $D^{*\prime +}$ production rate. $D^{*\prime}$ production is simulated in fragmentation and in B meson decays. In the latter case, the production channels for the $D^{*\prime}$ were chosen to be the same as those for the D_2^*, with equal branching fractions.

Four samples of $D^{*\prime}$ Monte Carlo events have been generated: production in $Z \to c\overline{c}$ and $Z \to b\overline{b}$ events and the decay channels $D^{*\prime +} \to D^{*+}\pi^+\pi^-$ and $D^{*\prime +} \to D_1^{\prime 0}\pi^+$. The signal Monte Carlo sample contains 600,000 events in total, with at least one charged $D^{*\prime}$ meson in each event. In all Monte Carlo samples, heavy quark fragmentation has been implemented using the the model of Peterson et al. [12] with fragmentation parameters determined from LEP data [13]. The samples have been passed through a detailed simulation of the OPAL detector [14] and then analyzed in the same manner as the data.

3 Event and Track Selection

Hadronic Z decays are selected based on the number of reconstructed tracks and the energy deposited in the electromagnetic calorimeter, as described in Ref. [15]. The analysis uses an initial sample of 3.73 million hadronic decays of the Z collected with the OPAL detector between 1991 and 1995.

Tracks are used in the reconstruction if they pass loose quality cuts requiring $|d_0| < 0.5$ cm, $|z_0| < 20$ cm, $p > 0.5$ GeV/c, and $p_{xy} > 0.150$ GeV/c. Here $|d_0|$ is the distance of closest approach of the track to the primary vertex, measured in the plane perpendicular to the beam, z_0 the distance along the beam at this point, p the momentum, and p_{xy} the momentum in the plane perpendicular to the beam. Only tracks with more than 40 hits out of a maximum of 159 in the main tracking chamber are used. The primary vertex in a collision is reconstructed from the tracks in the event and constrained by the known average position and spread of the e^+e^- interaction point. To improve the mass resolution, a track is required to have a precise z measurement at the exit point of the tracking chamber, either from an associated hit in the z-chamber surrounding the central drift chamber, or from the presampler. In cases where the particle exited the tracking chamber in the endcap region, i.e. $|\cos\theta| > 0.73$, the exit point is determined precisely from the last sense wire used for the track measurement.

4 Reconstruction of $D^{*\prime +}$ Candidates

The reconstruction of $D^{*\prime +} \to D^{*+}\pi^+\pi^-$ decays involves D^{*+} reconstruction and, subsequently, the combination of accepted D^{*+} candidates with additional pion candidates. The D^{*+} reconstruction follows closely a recent OPAL publication [16], with the exception of the cut on the kaon particle identification probability which has been tightened for this analysis, in order to reduce combinatorial background.

The following decay sequence is reconstructed exclusively:

$$
\begin{aligned}
\mathrm{D}^{*\prime +} \rightarrow & \mathrm{D}^{*+}\pi^+\pi^- \\
& \hookrightarrow \mathrm{D}^0\pi^+ \\
& \quad \hookrightarrow \mathrm{K}^-\pi^+
\end{aligned}
$$

All tracks that fulfil the criteria described in Section 3 are considered for the construction of $\mathrm{D}^{*\prime +}$ candidates. Only combinations of tracks that have the correct charge assignments, and which pass intermediate requirements imposed by the reconstruction of the D^{*+}, are taken into account. The two pions produced in the initial $\mathrm{D}^{*\prime +}$ decay will be referred to as "$\mathrm{D}^{*\prime +}$ pions", whereas the pion coming from the D^{*+} decay will be referred to as "slow pion".

Two tracks of opposite charge are accepted as a D^0 candidate if their invariant mass lies within the range $1.79-1.94$ GeV/c^2, assigning the pion mass to one particle and the kaon mass to the other [3]. D^0 candidates are combined with tracks of charge opposite to that of the kaon candidate to form D^{*+} candidates. The scaled energy x_E of the D^{*+} candidate, i.e. the ratio of the energy sum of all participating tracks over the beam energy, is required to be larger than 0.2 in order to reject combinatorial background from low-energy fragmentation tracks. The difference of the invariant masses of D^{*+} and D^0 candidates, $\Delta m = m_{\mathrm{D}^*} - m_{\mathrm{D}^0}$, must lie within the interval from 142 to 149 MeV/c^2.

Background in the sample is further reduced by cutting on the helicity angle θ^* measured between the direction of the D^0 candidate in the laboratory frame and the direction of the kaon in the rest frame of the D^0 candidate. The kaon candidate from the D^0 decay is expected to be isotropically distributed in $\cos\theta^*$, while the background peaks at $\cos\theta^* = -1$ and, particularly at small x_E, at $\cos\theta^* = +1$. This effect is taken into account by requiring $\cos\theta^* > -0.9$ for $x_\mathrm{E} > 0.5$ and $|\cos\theta^*| < 0.8$ for $x_\mathrm{E} < 0.5$.

At low x_E, where the background is most pronounced, the particle identification power of the OPAL detector is used to enrich the sample in true kaons from D^0 decays. A probability W_K is computed from the ionization energy loss measurement of a track in the drift chamber, the track momentum, and the theoretical expectation for a kaon. At least 20 $\mathrm{d}E/\mathrm{d}x$ out of a possible 159 measurement points and $W_\mathrm{K} > 10\%$ are required for the kaon candidate in a D^{*+} candidate with $x_\mathrm{E} < 0.5$.

A fraction (1.5%) of all D^{*+} candidates share the same slow pion candidate with another D^{*+} candidate in the same event. In this case only the D^{*+} candidate with a D^0 invariant mass closest to the mean value obtained from a fit to the D^0 mass distribution is kept for the further analysis. The D^{*+} candidates surviving the cuts described above are combined with all remaining pairs of oppositely charged tracks. For these combinations, a mass difference $\Delta m^{'} = m_{\mathrm{D}^{*\prime}} - m_{\mathrm{D}^*}$ is calculated.

In order to suppress background from uds events, charm and bottom tags are used. The mean fractional energy of $\mathrm{D}^{*\prime +}$ mesons in $\mathrm{Z} \rightarrow \mathrm{c\overline{c}}$ events is expected to be large compared to $\mathrm{D}^{*\prime +}$ from B decays, and especially compared to fake $\mathrm{D}^{*\prime +}$ candidates in events of all flavours consisting of low-energy fragmentation tracks. Since most of the energy of the $\mathrm{D}^{*\prime +}$ is transferred to the D^{*+}, a charm enriched sample is selected by imposing a cut on the energy fraction of the D^{*+} of $x_\mathrm{E} > 0.4$. Additionally, in the Monte Carlo simulation, the $\mathrm{D}^{*\prime +}$ pions have a higher momentum if the $\mathrm{D}^{*\prime}$ is produced in $\mathrm{c\overline{c}}$ events compared to the production via the

decay of b hadrons. This information has been exploited by selecting only candidates for which the magnitude of the vector sum of the two $D^{*\prime}$ pion momenta is greater than 3.6 GeV/c (Figure 1). The mass resolution in the charm enriched sample is improved by constraining all $D^{*\prime +}$ candidate tracks except those from the D^0 decay to the primary event vertex.

A bottom-enriched sample is selected by requiring an apparent D^0 decay length of at least 0.3 mm, defined as the distance between the reconstructed D^0 vertex and the primary event vertex, measured in the plane perpendicular to the beam. D^0 candidates from light quark (uds) events and $c\overline{c}$ events are expected to be made up from tracks in the vicinity of the primary vertex. In contrast, D^0 candidates in $b\overline{b}$ events tend to have a larger decay length with respect to the primary vertex, due to the B meson lifetime.

The separation significance of two vertices is defined as the distance between them in the plane perpendicular to the beam, divided by the uncertainty on this quantity. The separation significance of the D^0 vertex and the reconstructed vertex formed by the $D^{*\prime}$ pion tracks is required to be between -2.0 and $+4.0$. The distribution of this variable is not centred at zero, because the D^0 has a lifetime large enough to be observed. The separation significance between the $D^{*\prime +}$ pion vertex and the D^0 vertex is shown in Figure 2. A positive sign indicates that the D^0 vertex is farther from the primary interaction point than the $D^{*\prime +}$ pion vertex. Positive values are expected for signal, because the D^0 occurs later in the decay chain.

flavour	charm enriched	bottom enriched	combined sample
uds	12%	10%	11%
c	60%	15%	31%
b	28%	75%	58%

Table 2: *Flavour composition of the charm enriched, bottom enriched and combined Monte Carlo samples.*

The Monte Carlo flavour composition of the $D^{*\prime +}$ candidates passing all selection criteria is shown in Table 2. For $D^{*\prime +}$ mesons from primary charm and bottom quarks, the reconstruction efficiencies are estimated from Monte Carlo analysis to be 14.1% and 7.1%, respectively. The combined efficiency for $D^{*\prime +}$ from both sources is 11.4%, assuming equal rates for production in charm and bottom events. This assumption is motivated by the range of production rate ratios observed for $D^{*\pm}$ [16] and orbitally excited $D_J^{(*)0}$ mesons [11]. The analysis has also been performed with several other assumptions, and the dependence of the results on these different scenarios is included as a systematic error.

5 Selection Results

In order to maximize the expected sensitivity of the analysis, the charm and bottom enriched samples with 1765 and 3051 candidates, respectively, in the $\Delta m^{'} = \mathrm{m_{D^{*\prime}}} - \mathrm{m_{D^{*}}}$ region between 2.3 GeV/c^2 and 3.0 GeV/c^2 are merged into a combined sample. The overlap of 324 candidates between charm and bottom sample is taken into account; candidates that have been tagged as charm and bottom are used only once. This sample contains a total of 4492 $D^{*\prime +}$ candidates

in 2192 events. The results for the combined sample and the b and c enriched samples are discussed below.

The $\Delta m^{'}$ distribution of the combined charm and bottom enriched sample is shown in Figure 3a. No narrow resonance is observed anywhere in the $\Delta m^{'}$ region between 0.3 and 1.0 GeV/c^2, although the Monte Carlo simulation with a $D^{*\prime}$ production rate fixed at the value published by DELPHI [6] shows a clear signal (see Figure 3b). This is also separately true for the c and b enriched samples, shown in Figures 4 and 5, respectively. Shape and normalization of the background differ in data and simulation, especially in the b enriched sample. This is due to $D^{*\prime +}$ candidates in the Monte Carlo where one track is incorrectly assigned to the $D^{*\prime +}$ candidate. These candidates lead to a broad enhancement in the mass distribution. The mean scaled energy x_{E} of these candidates is small. Therefore, they contribute more to the b enriched sample than to the c enriched sample. The analysis has also been performed on a Monte Carlo sample without $D^{*\prime}(2629)$ production. It has been found that in this case the background shape and normalization agree very well with the data. This absence of a significant enhancement over the expected background in data provides additional confidence that the $D^{*\prime +}(2629)$ production rate must be small.

A limit on the $D^{*\prime +}(2629)$ production rate is calculated by defining a mass window in the $\Delta m^{'}$ range of 0.58 GeV/c^2 $< \Delta m^{'} <$ 0.66 GeV/c^2, corresponding to a $D^{*\prime}$ mass window of $2.59 - 2.67$ GeV/c^2. This includes the $\pm 2\sigma$ range of both the theoretical prediction of the $D^{*\prime}$ [2] and the excess observed by DELPHI [6]. The background distribution has been fitted using a parametrisation of the form [6, 11]

$$\mathrm{f}(\Delta m^{'}) = \alpha \, (\Delta m^{'} - m_0)^{\beta} \, \mathrm{e}^{-\gamma(\Delta m^{'} - m_0)} \, , \qquad (1)$$

where $m_0 = 0.28$ GeV/c^2 is the kinematic limit for $D^{*+}\pi^+\pi^-$ combinations, and α, β and γ are the fit parameters. The signal region has been excluded from the fit. The number of $D^{*\prime +}$ candidates in the mass window is determined to be 14 ± 28 by subtracting the integrated interpolated background function from the observed number of candidates in the signal interval. The quoted statistical error is obtained by combining the Gaussian variance of the number of entries in the mass window (± 25) and the uncertainty on the background integral obtained by propagating the uncertainties on the fit parameters (± 14), taking into account the correlations.

6 Systematic Checks

The $D^{*\prime +}$ analysis has been checked by applying a similar selection to $D^{*+}\pi^-$ final states, looking for the narrow orbital resonances D_1^0 and D_2^{*0}. The D^{*+} selection criteria are as described earlier. Accepted D^{*+} candidates are combined with pion candidates passing selection criteria similar to those applied to the $D^{*\prime +}$ pions, except for the cuts on the pion-pion momentum sum and the pion-pion vertex separation, which are inappropriate here. Instead, the pion momentum is required to be larger than 2.0 GeV/c, as was done in an earlier OPAL publication on orbitally excited D mesons [11]. The efficiency of the $D_J^{(*)0} \to D^{*+}\pi^-$ reconstruction is about 7.3%. The results achieved on data and simulated events can be compared in Figure 6. The method used for determining the number of signal events is the same as was used for the $D^{*\prime +}$. The lower mass window boundary has been set to 2.382 GeV/c^2, two D_1^0 widths below the world average

D_1^0 mass. The upper boundary has been chosen to be 2.507 GeV/c^2, two D_2^{*0} widths above the world average D_2^{*0} mass. The production rates of the two narrow $D_J^{(*)0}$ resonances have been adjusted in the simulation to match the previous OPAL measurement [11]. The amount of signal found in Monte Carlo is 281 ± 16, whereas in data the excess is 189 ± 41 in a sample of 4711 selected $D_J^{(*)0}$ candidates. The analysis presented here and the previous OPAL publication on orbitally excited D mesons [11] that was used to adjust the $D_J^{(*)0}$ production rates in Monte Carlo use a similar dataset. Both results are therefore expected to be correlated. Nevertheless, it has been found that the overlap of the selected $D_J^{(*)0}$ candidate samples of old and new analysis is very small, and the results can thus be considered almost statistically independent. This leads to the conclusion that the measured rates are statistically compatible.

Having confirmed in the case of $D^{*+}\pi^-$ final states that the reconstruction procedure performs as expected, the results of the search in the $D^{*+}\pi^+\pi^-$ final state are used to place limits on the production rate of the $D^{*\prime+}(2629)$. The efficiency of $D^{*\prime+}$ reconstruction is taken from Monte Carlo simulation. The efficiency calculation accounts for several sources of systematic uncertainties. They are evaluated as follows:

- The efficiency has been calculated from a simulation with zero $D^{*\prime+}$ width. To quantify the effect of a non-zero width, the analysis has been repeated with a $D^{*\prime+}$ width of 15 MeV/c^2, the 95% C.L. upper limit obtained by DELPHI [6]. This results in a relative decrease of the efficiency of 16.5%, taken as systematic uncertainty.

- The simulated detector resolutions of momentum, impact parameters and track angles have been varied by $\pm 10\%$, as in previous publications [11, 16], around the values that best describe the data. The largest relative deviation in the selection efficiency ($^{+4.9\%}_{-5.7\%}$) is taken as systematic uncertainty.

- Equal production rates of $D^{*\prime+}$ in c and b decays have been assumed. Other possible assumptions include the same ratio as observed in $D^{*\pm}$ production [16], or in $D_J^{(*)0}$ production [11]. Equal numbers of $D^{*\prime}$ from both primary heavy flavours are simulated as well as the ratio of candidates from $b\overline{b}$ and $c\overline{c}$ events observed by DELPHI [6], corrected for the different reconstruction efficiencies of the respective analyses. The ratios thus obtained cover a $^{+33\%}_{-23\%}$ range around the central assumption of equal production rates in $b\overline{b}$ and $c\overline{c}$ events. The largest observed variations in the efficiency in both directions, $^{+3.8\%}_{-4.6\%}$, are taken as systematic uncertainty.

- A Peterson function has been used to parametrise the heavy quark fragmentation in the Monte Carlo samples. Other fragmentation models by Collins and Spiller [17] and Kartvelishvili [18] have also been tested. The fragmentation parameters have been varied in the limits implied by the measurement of the mean x_E distribution of D^{*+} mesons at LEP [13]. The largest resulting uncertainty of $^{+1.7\%}_{-2.3\%}$ is taken as systematic uncertainty.

- The efficiency depends on the performance of the particle identification by $\mathrm{d}E/\mathrm{d}x$ measurements. The $\mathrm{d}E/\mathrm{d}x$ calibration for kaons has been checked in a previous analysis [19] under identical circumstances. An error of $\pm 3.2\%$ was found for the total rate of kaons passing the selection. Because this cut is applied only for candidates with $x_\mathrm{E} < 0.5$, the expected contribution to the uncertainty on the efficiency is $\pm 2.1\%$.

- The D^0 lifetime is currently measured with a precision of 0.7%, whereas the average b hadron lifetime is known to 0.9% [3]. The cut on the D^0 apparent decay length and thus the b flavour enrichment is sensitive to the modelling of this quantity. The cut value has therefore been varied within the combined uncertainty on D^0 and B lifetime. The resulting deviation of $^{+0.2\%}_{-0.0\%}$ is taken as systematic uncertainty.

- The calculated production limit depends on the branching ratio $\mathrm{Br}(D^{*+} \to D^0\pi^+) \times \mathrm{Br}(D^0 \to K^-\pi^+)$. The world average value is $(0.677 \pm 0.005) \times (0.0383 \pm 0.0009)$ [3]. The relative uncertainty on the product branching ratio is $\pm 2.5\%$.

- The reconstruction efficiencies of the decay chains $D^{*\prime +} \to D_1^{\prime 0}\pi^+$, $D_1^{\prime 0} \to D^{*+}\pi^-$ and $D^{*\prime +} \to D^{*+}\pi^+\pi^-$ are identical within the statistical uncertainties. No systematic uncertainty is introduced.

- The reconstructed number of $D^{*\prime +}$ in Monte Carlo has been compared to the actual number of $D^{*\prime +}$ in the sample. The excess over the background fit is 138 ± 30, with 175 entries due to $D^{*\prime +}$ with all tracks reconstructed. It is thus concluded that the fit is free of significant bias.

- The width of the signal region has been varied from 90% to 130% of the nominal value to check whether the resulting counting rate variations are consistent with statistical effects. All results are clearly within the statistical error. Thus no additional systematic uncertainty is assigned.

- The bin width of the m' histograms in which the fit is performed has been varied from 75% to 125% of the value used for the analysis. No significant impact on the rate is observed.

The contributions to the systematic uncertainty are summarized in Table 3.

7 Calculation of $D^{*\prime\pm}(2629)$ Production Limits

The limit is calculated assuming that the candidate sample in the signal region is composed of a large background and a small signal sample. Each contribution has a Poisson probability density function although the background can be approximated by a Gaussian distribution $\mathcal{G}(n; e_{\mathrm{bck}}, \sigma)$ since the background expectation is large. The width of the Gaussian, $\sigma = 28$, has two contributions, one accounting for the statistical uncertainty in the signal window, the other one taking into account the fit error. $n_0 = 610$ candidates are observed in the signal window. The probability to count n_0 candidates or less is given by

$$P(n_0; e_{\mathrm{sig}}) \;=\; \sum_{n=0}^{n_0} \sum_{n_{\mathrm{sig}}=0}^{n} \mathcal{P}(n_{\mathrm{sig}}; e_{\mathrm{sig}})\; \mathcal{G}(n - n_{\mathrm{sig}}; e_{\mathrm{bck}}, \sigma) \tag{2}$$

where e_{sig} is the unknown expectation value of the signal and $\mathcal{P}$ its Poisson distribution. The summation is performed over all possible combinations of n, the total number of candidates in the mass window, and n_{sig}, the amount of signal within these n candidates, where $n \leq n_0$. Assuming no narrow $D^{*\prime +}$ are produced, i.e. $e_{\mathrm{sig}} = 0$, a probability of 0.70 is obtained to observe

error source	relative contribution		
	c enriched	b enriched	combined
relative errors on Monte Carlo efficiency			
$D^{*\prime+}$ width	$^{+0.0\%}_{-17.9\%}$	$^{+0.0\%}_{-10.6\%}$	$^{+0.0\%}_{-16.5\%}$
detector resolution	$^{+5.2\%}_{-6.1\%}$	$^{+4.5\%}_{-5.7\%}$	$^{+4.9\%}_{-5.7\%}$
relative production rates in b and c	none	none	$^{+3.8\%}_{-4.6\%}$
fragmentation modelling	$^{+3.6\%}_{-3.7\%}$	$^{+1.1\%}_{-0.3\%}$	$^{+1.7\%}_{-2.3\%}$
kaon $\mathrm{d}E/\mathrm{d}x$	$^{+1.3\%}_{-1.3\%}$	$^{+2.6\%}_{-2.6\%}$	$^{+2.1\%}_{-2.1\%}$
B and D^0 lifetimes	none	$^{+0.5\%}_{-0.0\%}$	$^{+0.2\%}_{-0.0\%}$
Monte Carlo statistics	$^{+0.1\%}_{-0.1\%}$	$^{+0.08\%}_{-0.08\%}$	$^{+0.07\%}_{-0.07\%}$
total	$^{+6.5\%}_{-19.3\%}$	$^{+5.3\%}_{-12.3\%}$	$^{+6.8\%}_{-18.4\%}$
relative errors on external branching ratios			
branching ratio $D^{*+} \to D^0\pi^+$, $D^0 \to K^-\pi^+$	$\pm 2.5\%$	$\pm 2.5\%$	$\pm 2.5\%$
error on $\Gamma_{b\overline{b}}/\Gamma_{\mathrm{had}}$ and $\Gamma_{c\overline{c}}/\Gamma_{\mathrm{had}}$	$\pm 2.9\%$	$\pm 0.3\%$	none
total	$^{+7.5\%}_{-19.7\%}$	$^{+5.9\%}_{-12.6\%}$	$^{+7.2\%}_{-18.6\%}$

Table 3: *Overview of the systematic error sources contributing to the total uncertainty.*

610 candidates or less. Given the prior knowledge of the maximum amount of background, the 95% C.L. limit is obtained at $P(n_0; e_{\mathrm{sig}}) = 0.70 \times 0.050$. At large n (≈ 10) the systematic uncertainties affecting the efficiency start playing a role in calculating the limit. They are considered by substituting the Poisson distribution of the signal with a Gaussian distribution at $n > 10$ and adding in quadrature the asymmetric systematic uncertainty of the efficiency to the width of the Gaussian given by $\sqrt{n}$. The limit obtained is:

$$f(\mathrm{Z} \to \mathrm{D}^{*\prime\pm}(2629)) \times \mathrm{Br}(\mathrm{D}^{*\prime+} \to \mathrm{D}^{*+}\pi^+\pi^-) < 3.1 \times 10^{-3} \quad (95\%\ \mathrm{C.L.}). \tag{3}$$

This corresponds to a 95% C.L. upper limit of 66 on the number of reconstructed $D^{*\prime+}$ in the signal region. The approach used here is similar to a Bayesian approach with a flat prior distribution for positive $D^{*\prime+}$ production rates and zero elsewhere, but superior in the fact that negative expectation values are excluded in principle by using the proper Poisson distribution.

Limits on the $D^{*\prime+}(2629)$ production rate in charm and bottom events are also calculated. In the charm and bottom enriched samples, the numbers of events in the signal region, relative to the expectations derived from the fitted background functions, are 5 ± 18 and 29 ± 23, respectively. In using these results to calculate limits, a further systematic uncertainty arises due to the experimental uncertainties on $\Gamma_{c\overline{c}}/\Gamma_{\mathrm{had}} = 0.1671 \pm 0.0048$ and $\Gamma_{b\overline{b}}/\Gamma_{\mathrm{had}} = 0.21644 \pm 0.00075$ [3]. Under the conservative assumption that $D^{*\prime+}$ are only produced in $\mathrm{Z} \to c\overline{c}$ events, i.e. that the measured excess can be fully assigned to $D^{*\prime+}$ candidates in $c\overline{c}$ events, a production limit of

$$f(\mathrm{c} \to \mathrm{D}^{*\prime+}(2629)) \times \mathrm{Br}(\mathrm{D}^{*\prime+} \to \mathrm{D}^{*+}\pi^+\pi^-) < 0.9 \times 10^{-2} \quad (95\%\ \mathrm{C.L.}) \tag{4}$$

is obtained from the charm enriched sample, while under the opposite assumption that all $D^{*\prime+}$

are only produced in the decay of b-hadrons, a limit of

$$f(\mathrm{b} \to \mathrm{D}^{*\prime +}(2629)) \times \mathrm{Br}(\mathrm{D}^{*\prime +} \to \mathrm{D}^{*+}\pi^+\pi^-) < 2.4 \times 10^{-2} \quad (95\%\ \mathrm{C.L.}) \tag{5}$$

is computed using the bottom enriched sample. The systematic uncertainties assumed for the calculations in the separate samples are given in Table 3.

8 Discussion

The result of the OPAL $\mathrm{D}^{*\prime +}$ search does not agree with the published DELPHI results [6]. Both analyses apply standard selection criteria to obtain a high-purity D^{*+} sample. In contrast to the OPAL analysis, DELPHI reconstructs D^0 candidates in two decay channels, $\mathrm{D}^0 \to \mathrm{K}^-\pi^+$ and $\mathrm{D}^0 \to \mathrm{K}^-\pi^+\pi^+\pi^-$. The loss in efficiency associated with using only the $\mathrm{K}^-\pi^+$ channel is in part compensated by the softer kinematic cuts and a slightly larger hadronic event sample. Combinatorial background is reduced by applying a best candidate selection to D^{*+} candidates which share tracks. These candidates can produce correlated entries in the $\Delta m^{'}$ distribution if they are combined with the same $\mathrm{D}^{*\prime +}$ pions. The expected sensitivity of the analysis to the existence of a narrow resonance in the mass region including the theoretical predictions for the $\mathrm{D}^{*\prime}$ as well as the mass of the published DELPHI result, produced at a rate published by DELPHI, is demonstrated in Figure 3. The excess observed in the Monte Carlo sample with comparable size to the data sample has a significance of 4.7σ (statistical error only), or 3.5σ including all systematic uncertainties.

The OPAL and DELPHI selection criteria used to select charm and bottom enriched samples, and for the pions from the $\mathrm{D}^{*\prime +}$ decay, have been optimized in different ways. For example, the kinematic cuts for the pion candidates from the $\mathrm{D}^{*\prime +}$ are less restrictive, 0.5 GeV/c in this analysis while DELPHI requires 1.0 GeV/c.

The sensitivity of the OPAL analysis has been checked with the $\mathrm{D}_J^{(*)0}$ reconstruction described above, where agreement between data and simulation is observed. The selection criteria that are specific to either the $\mathrm{D}^{*\prime +}$ or $\mathrm{D}_J^{(*)0}$ analysis are checked by performing the analysis without these cuts. This did not change the result of the $\mathrm{D}^{*\prime +}$ search.

Overall, the sensitivities of the two analyses are found to be similar, although the background in this analysis is higher. A comparison between the analyses can be made by calculating the $\mathrm{D}^{*\prime +}$ versus $\mathrm{D}_J^{(*)0}$ rate for which DELPHI published a number [6]:

$$\begin{aligned} R &= \frac{\langle N_{\mathrm{D}^{*\prime +}} \rangle \mathrm{Br}(\mathrm{D}^{*\prime +} \to \mathrm{D}^{*+}\pi^+\pi^-)}{\langle N_{\mathrm{D}_1^0} \rangle \mathrm{Br}(\mathrm{D}_1^0 \to \mathrm{D}^{*+}\pi^-) + \langle N_{\mathrm{D}_2^{*0}} \rangle \mathrm{Br}(\mathrm{D}_2^{*0} \to \mathrm{D}^{*+}\pi^-)} \\ &= 0.49 \pm 0.18(\mathrm{stat.}) \pm 0.10(\mathrm{syst.})\ , \end{aligned} \tag{6}$$

where $\langle N_{\mathrm{D}^{*\prime +}} \rangle$ denotes the expected number of $\mathrm{D}^{*\prime +}$ in a sample with $\langle N_{\mathrm{D}_1^0} \rangle$ and $\langle N_{\mathrm{D}_2^{*0}} \rangle$ being the corresponding quantities for the D_1^0 and D_2^{*0}. Based on the numbers presented in Sections 5 and 6,

$$R = 0.05 \pm 0.10(\mathrm{stat.}) \pm 0.002(\mathrm{syst.}) \tag{7}$$

is calculated. The statistical error of the fit and the systematic uncertainties resulting from the $\mathrm{D}^{*\prime}$ width and relative production rates in b and c are included. In the ratio calculation,

all other systematic uncertainties largely cancel and have therefore been neglected. Using a statistical approach analogous to the one described earlier, a limit of

$$R < 0.22 \quad (95\% \text{ C.L.}) \tag{8}$$

is computed.

In summary, the evidence of $D^{*\prime +}$ production in hadronic decays of the Z published by the DELPHI collaboration [6] is not confirmed with OPAL data.

Acknowledgements

We particularly wish to thank the SL Division for the efficient operation of the LEP accelerator at all energies and for their continuing close cooperation with our experimental group. We thank our colleagues from CEA, DAPNIA/SPP, CE-Saclay for their efforts over the years on the time-of-flight and trigger systems which we continue to use. In addition to the support staff at our own institutions we are pleased to acknowledge the
Department of Energy, USA,
National Science Foundation, USA,
Particle Physics and Astronomy Research Council, UK,
Natural Sciences and Engineering Research Council, Canada,
Israel Science Foundation, administered by the Israel Academy of Science and Humanities,
Minerva Gesellschaft,
Benoziyo Center for High Energy Physics,
Japanese Ministry of Education, Science and Culture (the Monbusho) and a grant under the Monbusho International Science Research Program,
Japanese Society for the Promotion of Science (JSPS),
German Israeli Bi-national Science Foundation (GIF),
Bundesministerium für Bildung und Forschung, Germany,
National Research Council of Canada,
Research Corporation, USA,
Hungarian Foundation for Scientific Research, OTKA T-029328, T023793 and OTKA F-023259.

References

[1] S. Godfrey, N. Isgur, Phys. Rev. **D32** (1985) 189.

[2] D. Ebert, V.O. Galkin, R.N. Faustov, Phys. Rev. **D57** (1998) 5663.

[3] Particle Data Group, D.E. Groom et al., Eur. Phys. J. **C15** (2000) 1.

[4] R. Kokoski, N. Isgur, Phys. Rev. **D35** (1987) 907; as quoted in [6].

[5] CLEO Collaboration, S. Anderson et al., Nucl. Phys. **A663–664** (2000) 647.

[6] DELPHI Collaboration, P. Abreu et al., Phys. Lett. **B426** (1998) 231.

[7] D. Melikhov, O. Péne, Phys. Lett. **B446** (1999) 336;
P.R. Page, Phys. Rev. **D60** (1999) 057501.

[8] OPAL Collaboration, K. Ahmet et al., Nucl. Instr. Meth. **A305** (1991) 275;
P.P. Allport et al., Nucl. Instr. Meth. **A324** (1993) 34;
P.P. Allport et al., Nucl. Instr. Meth. **A346** (1994) 476;
O. Biebel et al., Nucl. Instr. Meth. **A323** (1992) 169;
M. Hauschild et al., Nucl. Instr. Meth. **A314** (1992) 74.

[9] T. Sjöstrand, Comp. Phys. Comm. **82** (1994) 74.

[10] OPAL Collaboration, G. Alexander et al., Z. Phys. **C69** (1996) 543.

[11] OPAL Collaboration, K. Ackerstaff et al., Z. Phys. **C76** (1997) 425.

[12] C. Peterson et al., Phys. Rev. **D27** (1983) 105.

[13] The LEP collaborations, ALEPH, DELPHI, L3 and OPAL,
Nucl. Instr. Meth. **A378** (1996) 101.

[14] J. Allison et al., Nucl. Instr. Meth. **A317** (1991) 47.

[15] OPAL Collaboration, R. Akers et al., Z. Phys. **C65** (1995) 17.

[16] OPAL Collaboration, K. Ackerstaff et al., Eur. Phys. J. **C1** (1998) 439.

[17] P. Collins, T. Spiller, J. Phys. **G11** (1985) 1289.

[18] V.G. Kartvelishvili, A.K. Likhoded, V.A. Petrov, Phys. Lett. **B78** (1978) 615.

[19] OPAL Collaboration, G.Abbiendi et al., Eur. Phys. J. **C13** (2000) 1.

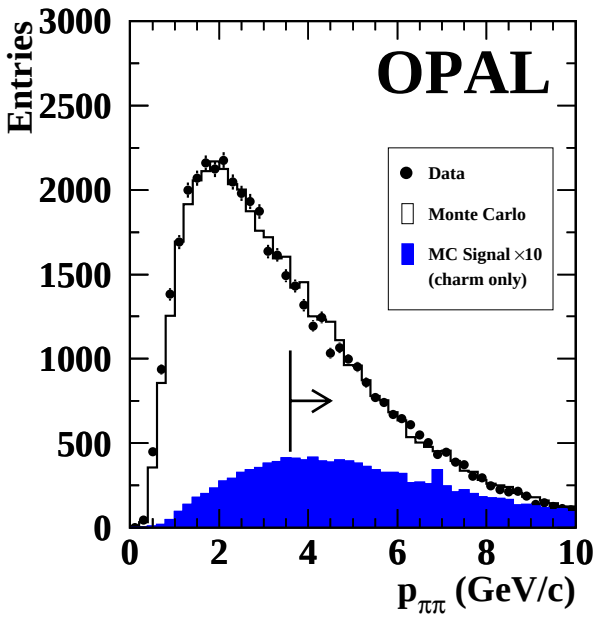

Figure 1: *Magnitude of the vector sum of the* $D^{*\prime}$ *pion momenta,* $p_{\pi\pi}$*, for data (points with error bars), Monte Carlo (open histogram, scaled to the same number of entries as data) and true* $D^{*\prime+}$ *(shaded, scaled up by a factor of 10). The arrow indicates the selected region.*

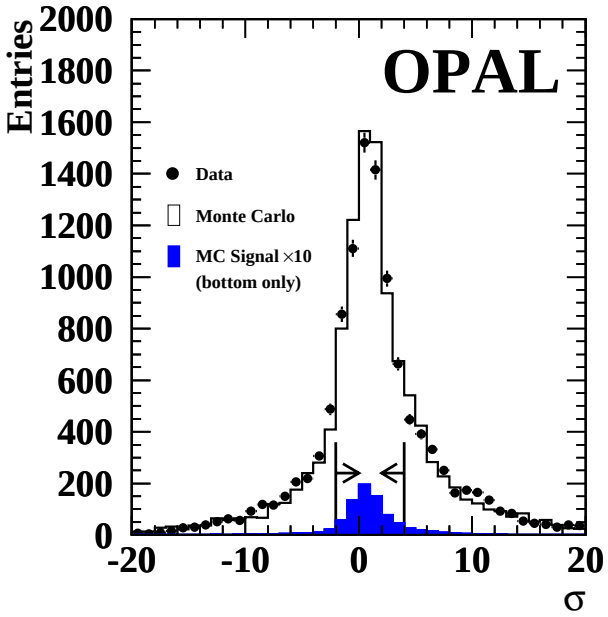

Figure 2: *Separation significance* σ *between the* D^0 *vertex and the reconstructed vertex of the* $D^{*\prime+}$ *decay pion tracks for data (points with error bars), Monte Carlo (open histogram, scaled to the same number of entries as data) and true* $D^{*\prime+}$ *(shaded, scaled up by a factor of 10) for candidates passing all selection criteria except for the cut on the quantity shown here. The arrows indicate the selected region.*

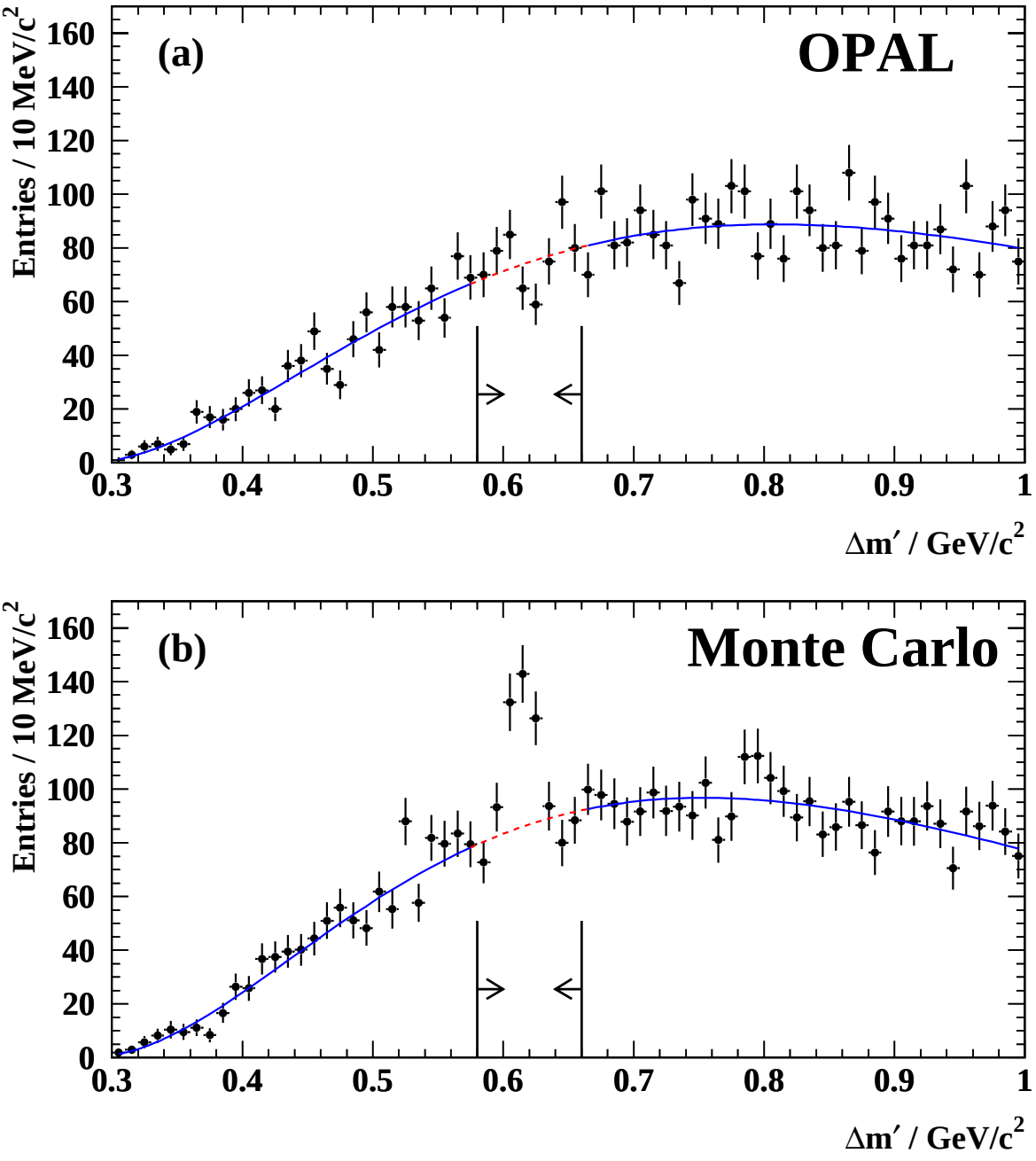

Figure 3: *Distribution of the mass difference* $\Delta m' = m_{\mathrm{D}^{*\prime}} - m_{\mathrm{D}^*}$ *of* $\mathrm{D}^{*\prime +}$ *candidates in the combined charm and bottom sample, for (a) data and (b) Monte Carlo. The calculation of* $\Delta m'$ *as well as the background parametrisation superimposed on the histogram are described in the text. The Monte Carlo histogram is scaled to the number of hadronic events in data. Furthermore, the* D^{*+} *Monte Carlo production rate has been adjusted to an OPAL measurement of this quantity [16], and the* $\mathrm{D}^{*\prime +}$ *production rate has been fixed at the value published by DELPHI [6] and the OPAL* $\mathrm{D}_J^{(*)0}$ *measurement [11]. The Monte Carlo plot presented here is created from a subsample of the available events that has roughly the same size as the data sample. The arrows indicate the mass window defined as the signal region. The line represents the result of the background fit, where the line is dashed in regions that have been excluded from the fit. The* χ^2*/dof of the background fit is 1.23 for data, and 0.99 for the Monte Carlo simulation.*

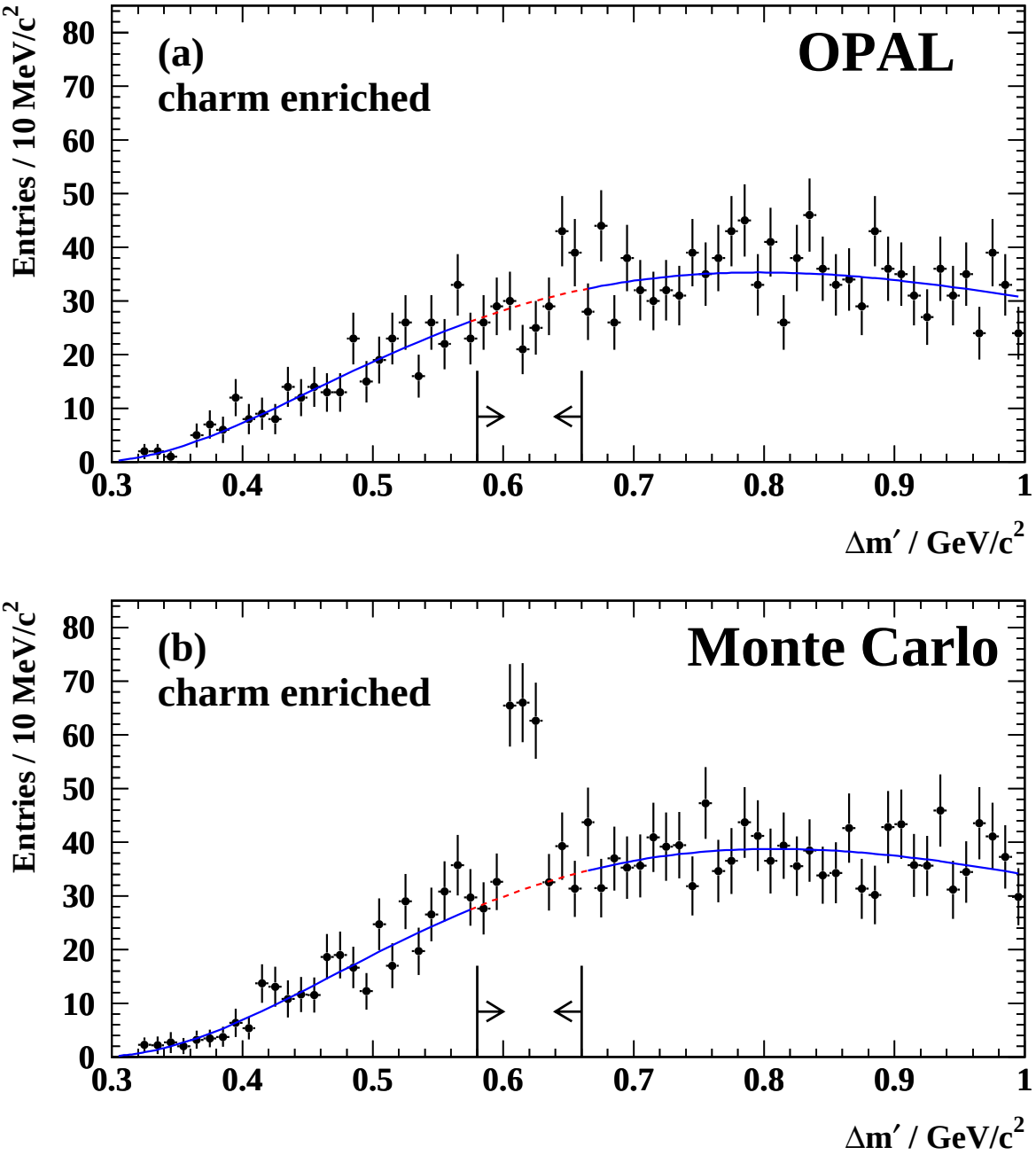

Figure 4: *Distribution of the mass difference* $\Delta m' = m_{\mathrm{D}^{*\prime}} - m_{\mathrm{D}^*}$ *of* $\mathrm{D}^{*\prime +}$ *candidates in the charm enriched sample, for (a) data and (b) Monte Carlo. The* χ^2*/dof of the background fit is 0.80 for data, and 0.70 for the Monte Carlo simulation.*

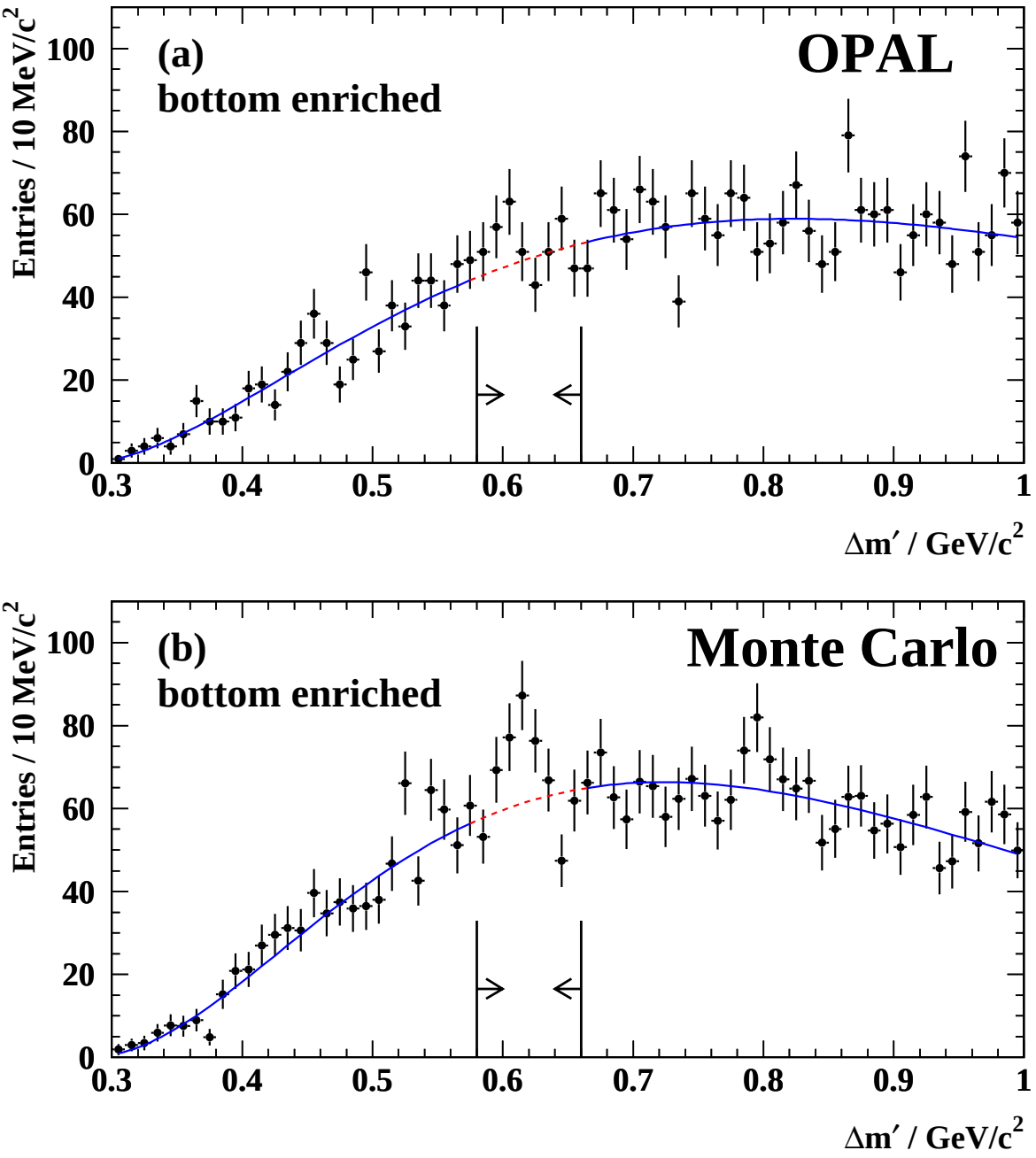

Figure 5: *Distribution of the mass difference* $\Delta m' = m_{\mathrm{D}^{*\prime}} - m_{\mathrm{D}^*}$ *of* $\mathrm{D}^{*\prime +}$ *candidates in the bottom enriched sample, for (a) data and (b) Monte Carlo. The* χ^2*/dof of the background fit is 1.20 for data, and 1.07 for the Monte Carlo simulation. The difference in shape and normalization of the background is explained by a large number of partially reconstructed* $\mathrm{D}^{*\prime +}$ *candidates which, due to their low mean scaled energy, mainly contribute to the b enriched sample. The analysis has also been performed on a Monte Carlo sample without* $\mathrm{D}^{*\prime}(2629)$ *production. It has been found that in this case the background shape and normalization agree very well with the data.*

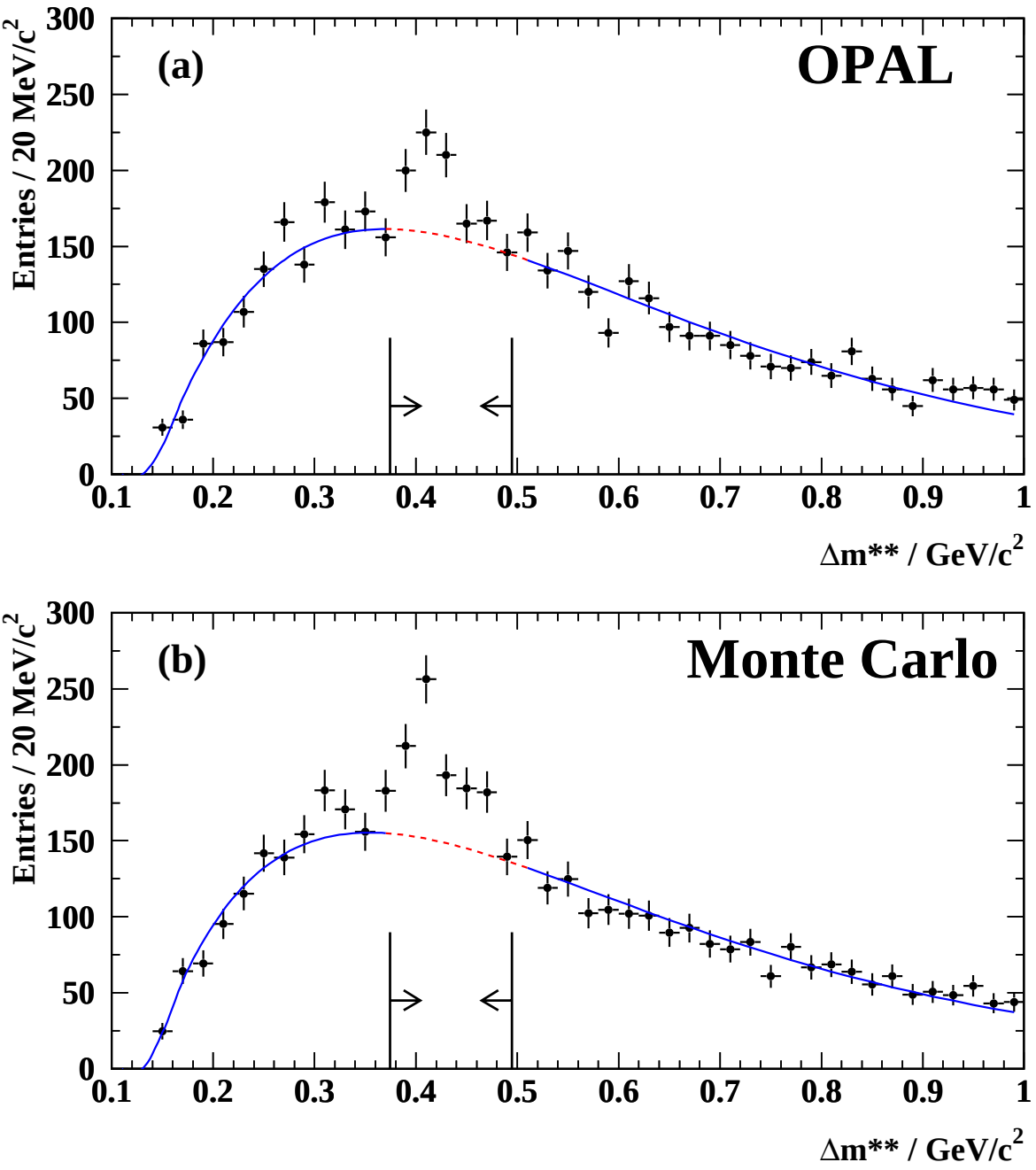

Figure 6: *Distribution of the mass* $\Delta m_{**} = m_{\mathrm{D}^{*+}\pi^-} - m_{\mathrm{D}^{*+}}$*, for (a) data and (b) Monte Carlo. The production rates of* $\mathrm{D}_J^{(*)0}$ *mesons in the Monte Carlo have been adjusted to the values measured in data [11]. The same parametrisation as in the* $\mathrm{D}^{*\prime +}$ *analysis is used to describe the background. The* χ^2*/dof of the fit is 1.43 for data, and 1.22 for the Monte Carlo simulation. The Monte Carlo histogram is scaled to the number of hadronic events in data.*